CyAbrB2 in *Synechocystis* sp. PCC6803 is a cyanobacterial nucleoid-associated protein controlling the expression of hydrogenase under the fermentative condition

Ryo Kariyazono[a] and Takashi Osanai[a]*

[a] School of Agriculture, Meiji University, 1-1-1 Higashimita, Tama-ku, Kawasaki, Kanagawa 214-8571, Japan

*Corresponding author: Takashi Osanai
Meiji University, 1-1-1 Higashimita, Tama-ku, Kawasaki, Kanagawa 214-8571, Japan
Tel: +81-44-934-7103; Fax: +81-44-934-7103; e-mail: tosanai@meiji.ac.jp

Key words:
Cyanobacteria; nucleoid associated proteins; hydrogenase; *Synechocystis* sp. PCC 6803; transcription

Summary

Cyanobacteria, the oxygenic photosynthetic bacteria, possesses Bi-directional hydrogenase (encoded by *hox* genes), which produces fermentative H_2, under the microoxic condition. The expression of a *hox* operon is elevated during microxic condition and genetic analyses on model cyanobacterium *Synechocystis* sp. PCC 6803 revealed that some global transcriptional regulators govern *hox* expression, but their dynamics are unknown. We here show that cyAbrB2, the repressor of *hox* operon, binds to hox promoter at the aerobic condition. In the microoxic condition, cyAbrB2 at hox promoter declined, and alternative sigma factor SigE became accessible to the promoter. We also revealed that cyAbrB2 broadly binds to AT-rich genome regions and represses expression from binding regions, which resembles nucleoid-associated proteins (NAPs). From the analogy to NAPs, we propose that cyAbrB2 mediates chromosomal conformation of hox promoter, which is relaxed under the microoxic condition, and thus fermentative genes are expressed.

Introduction

Cyanobacteria carry out oxygenic photosynthesis converting CO_2 to carbohydrates and storing them as glycogen. Stored glycogen is catabolized via glycolysis and respiration during nighttime. Cyanobacteria sometimes experience microoxic conditions during the night due to respiration. (Stal and Moezelaar, 1997). Then cyanobacteria utilize glycolytic products as electron acceptors to replenish oxidized cofactors required for glycolysis. This process is called fermentation, and cyanobacteria possess multiple fermentation pathways. For example, a euryhaline cyanobacterium *Synechococcus* sp. PCC7002 procedures lactate, hydrogen, alanine, succinate, and acetate under the dark microoxic condition (McNeely et al., 2010), and freshwater living cyanobacterium *Synechocystis* sp. PCC6803 (hereafter referred to as *Synechocystis*) produces acetate, lactate, dicarboxylic acids, and hydrogen (Osanai et al., 2015; Stal and Moezelaar,

1997). Cyanobacteria coordinate the activity of each pathway according to the environment because each fermentation pathway has a different ATP gain, redox balance, and substrate availability. Genetic manipulations on *Synechocystis* revealed that changing expression level of some enzymes could alter fermentative metabolic flow (Iijima et al., 2016, 2021), supporting the notion that transcription regulates the fermentative pathway.

Among cyanobacterial bioproducts, hydrogen is attractive as the application for biofuel and has been intensively studied so far. H_2 production from protons is catalyzed by bi-directional hydrogenase (Carrieri et al., 2011), which is distributed commonly among cyanobacteria except for open ocean habitants (Puggioni et al., 2016). NADH, reduced ferredoxin, and flavodoxin can be substrates for the bi-directional hydrogenase (Gutekunst et al., 2014). Cyanobacterial hydrogenase comprises five subunits (HoxEFUHY) and contains Nickel and Fe-S clusters, and auxiliary proteins (HypABCDEF) help assemble the complex (Cassier-Chauvat et al., 2014). In addition to fermentative H_2 production, hydrogenase utilizes excess electron from the photosynthetic electron transport chain, though oxygen generated by photosystem II inactivate hydrogenase (Appel et al., 2000). Pyruvate-ferredoxin oxidoreductase (PFOR) is another metal-ion-harboring and O_2-sensitive enzyme. PFOR oxidates pyruvate and produces acetyl-CoA under fermentative conditions. PFOR and hydrogenase work in a coupled manner; PFOR reduces ferredoxin, which hydrogenase uses as the electron donor (Gutekunst et al., 2014). Due to its sensitivity to O_2 and requirement for metal ions, untimely or excess production of hydrogenase and PFOR should lead to futile inactive enzymes. Therefore, transcriptional regulation responding to the environment is essential for optimal energy cost performance.

Promoter recognition by RNA polymerases is the essential step for transcriptional regulation. Sigma factors, a subunit of RNA polymerase, recognize core promoter sequences. Transcription factors also bind promoter regions and suppress or promote transcription by RNA polymerase. In addition, transcription factors called nucleoid-associated proteins (NAPs) regulate transcription by modulating chromosomal conformation, although cyanobacterial NAPs have been

elusive. The coding genes of HoxEFUHY form a single operon (*sll1220-1226*), and PFOR is encoded in *nifJ* (*sll0741*) gene in *Synechosysits*. *Hox* operon and *nifJ* are highly expressed in microoxic conditions (Summerfield et al., 2011). Genetic analysis revealed that multiple global transcriptional regulators control the expression of *hox* and *nifJ*. Sigma factor SigE(Sll1689) is responsible for the expression of *hox* and *nifJ* operons (Osanai et al., 2005, 2011), and transcription factor cyAbrB2(Sll0822) represses them (Dutheil et al., 2012; Leplat et al., 2013). LexA(Sll1626) and cyAbrB1(Sll0329) are positive regulators for *hox* operon (Gutekunst et al., 2005; Oliveira and Lindblad, 2005, 2008).

SigE is an alternative sigma factor that governs the expression of glycogen catabolism and glycolysis, including PFOR/*nifJ* and hydrogenase (Osanai et al., 2005). SigE shows high amino acid sequence homology to primary sigma factor SigA, which transcribes housekeeping and photosynthetic genes (Imamura and Asayama, 2009). ChIP-seq study revealed that most SigE binding sites are the same as SigA, but promoters of glycogen catabolism and glycolysis are exclusively occupied by SigE (Kariyazono and Osanai, 2022).

CyAbrB2 and cyabrB1 are highly conserved transcription factors in cyanobacteria. CyAbrB2 regulates the expression of many genes, including carbon metabolism, nitrogen metabolism, and cell division (Ishii and Hihara, 2008; Leplat et al., 2013; Lieman-Hurwitz et al., 2009). CyAbrB2 binds *hox* promoter in vitro and represses its expression in vivo (Dutheil et al., 2012). CyAbrB1 is an essential gene and physically interacts with the cyAbrB2 protein(Yamauchi et al., 2011). CyAbrB1 also binds to *hox* promotor region in vitro and promotes its expression (Oliveira and Lindblad, 2008).

SigE, LexA, cyAbrB2, and cyAbrB1 are expected to bind or dissociate dynamically to *hox* promoter region in response to the microoxic condition. However, the dynamism of transcriptional regulators upon entry into the microoxic condition is poorly understood. Here we conducted a time-course analysis of transcriptome and ChIP-seq of SigE and cyAbrB2 on entry to microoxic condition. We found that *hox* and *nifJ* operons showed transient upregulation behaving distinctly from other microoxic up-regulated genes. SigE and cyAbrB2 predominantly control the transiently up-regulated genes. ChIP-

seq revealed that cyAbrB2 binds to long tracts of AT-rich regions in the genome and represses expression from its binding regions at aerobic conditions. Our observation showed that the behavior of cyAbrB2 resembles NAPs. The binding regions of cyAbrB2 include the promoter and gene body of *hox* and *nifJ*. Interestingly, cyAbrB2 binding to *hox* and *nifJ* promoters became less specific under the microoxic condition, and SigE binding to *hox* and *nifJ* promoters became prominent. We propose cyAbrB2 modulates chromosome conformation like NAPs, allowing access of SigE-containing RNA polymerase complex.

Result

Transcriptomes on entry to dark microoxic conditions

To understand the transcriptional regulation under microoxic condition, we conducted time-course transcriptome capturing aerobic and 1, 2, and 4 hr after microoxic conditions (Figure 1A). The gene set enrichment analysis comparing the aerobic and microoxic conditions revealed that many biological pathways, including photosynthesis and respiration (oxidative phosphorylation), are downregulated (Figure 1B). Up-regulated pathways include butanoate metabolism and two-component systems, but the actual cyanobacterial catabolic pathway slightly differs from that described in the KEGG pathway. 508 genes showed more than 2-fold increase within 1hr switching from aerobic to anaerobic conditions. We further classified genes with increased expression into four classes according to time course (Figure 1C). Out of 508 genes, 28 were defined as “transiently up-regulated genes” because they showed decreased expression upon the comparison of 1-hour and 4-hour incubation under microoxic conditions (log2 fold change < -0.5). 199 in 508 genes continuously increased between 1hr and 4hr incubation under the microoxic condition (log2 fold change > 0.5), and we termed them as “continuously up-regulated genes.” When we mapped classified genes to central carbon metabolism, *nifJ* encoding pyruvate-ferredoxin oxidoreductase (PFOR) and *hox* operon encoding bidirectional hydrogenase complex

showed transient upregulation (Figure 1D and Table 1).

SigE and cyAbrB2 control the expressions of transiently up-regulated genes

The functional correlation between hydrogenase and PFOR, encoded by *hox* operon and *nifJ*, respectively, implies that transient upregulation has physiological significance. We focused on transiently up-regulated genes and attempted to reveal the regulatory mechanism of transient upregulation. Previous studies showed that transcription factor LexA, cyAbrB1, and alternative sigma factor SigE positively regulate the expression of hox operon, while transcription factor cyAbrB2 is a suppressor (Dutheil et al., 2012). SigE also promotes *nifJ* expression, and cyAbrB2 represses *nifJ*. Thus, we made *Synechocystis* mutants whose SigE or cyAbrB2 are genetically disrupted (Figure S1A) and conducted time-course transcriptome analysis (the aerobic condition, 1hr and 2hr cultivation of dark microoxic conditions) on those disruptants. (Figure 2A) The transcriptome data reproduced that the expression of *hox* operon is controlled by SigE and cyAbrB2 (Figure 2B). We searched differentially expressed genes between mutants and wildtype (more than 2-fold expression change with less than 0.05 of FDR) in each time point and found that deletion of either SigE and cyAbrB2 preferentially affected the expression of transiently up-regulated genes (Figures 2C and 2D). Curiously, the deletion of cyAbrB2 caused up-regulated transient genes under the aerobic condition in contrast to that under 1hr cultivation in the microoxic condition (Figure 2C).

Genome-wide analysis of cyAbrB2, cyAbrB1, and SigE via ChIP-seq

Prior to revealing the regulation mechanism of transiently up-regulated genes, we had to understand those transcriptional regulators' universal features and functions. For this purpose, we surveyed the genome-wide occupation of cyAbrB2 and SigE (Figures S1 and S2) and compared it with transcriptome data. In detail, we made *Synechocystis* strain whose cyAbrB2 is epitope-tagged and conducted ChIP-seq assay under aerobic and microoxic conditions (Figures S1B and S1C). We used SigE-tagged strains previously constructed and analyzed elsewhere (Kariyazono and Osanai,

2022). Primary sigma factor SigA is also analyzed to determine SigE-specific binding. In addition to cyAbrB2, we made tagged cyAbrB1, the interactor of cyAbrB2 and positive regulator of *hox* operon.

CyAbrB2 binds to long tracts of the genomic region and suppresses genes in the binding region

ChIP-seq data of Flag-tagged cyAbrB2 show that cyAbrB2 bound long tracts of the genomic region, and its binding regions showed lower GC contents than the whole genome *Synechocystis* (Figures 3A and 3B). Conversely, regions with lower GC contents showed greater binding signal of cyAbrB2 (Figure 3C). This is not a systematic bias of NGS because the binding signal of SigE, SigA, and control did not show such a negative correlation to GC contents (Figure S3A). 805 of 3614 genes overlapped with cyAbrB2 binding regions, and almost half (399 of 805 genes) were entirely covered by the cyAbrB2 binding region. CyAbrB2 binding regions include 80 of 125 insertion sequence elements (Figure 3D). The comparison with the transcriptome of *cyabrB2*Δ revealed that genes overlapping with cyAbrB2 binding regions tend to be suppressed by cyAbrB2 in aerobic conditions (Figures 3A and 3E). We also surveyed the genomic localization of cyAbrB1 in the aerobic condition. We found that the binding pattern of cyAbrB1 is similar to that of cyAbrB2 (Figures 3A and S3B). Due to the essentiality of cyAbrB1, we did not conduct transcriptome of the cyAbrB1 disrupted strain. When cells entered the microoxic condition, relative binding signals in cyAbrB2 binding regions generally declined (Figure S4A). Considering that the relative signal is normalized by total IP reads, the signal change does not necessarily mean that binding of cyAbrB2 declined in the microoxic condition. Instead, the binding pattern of cyAbrB2 became uniform when cells entered the microoxic condition. Actually, total quantities of precipitated DNA by tagged cyAbrB2 were not decreased (Figure S4B) ,and qPCR confirmed that cyAbrB2 binding signal increased in all positions tested (Figure S4C).

cyAbrB2 binds to transiently up-regulated genes

Binding regions of cyAbrB2 overlapped 17 of 28 transiently up-regulated genes, showing significant enrichment from

all up-regulated genes (Figure 3F). While cyAbrB2 covers the entire length of transposons and unknown proteins, the binding positions of cyAbrB2 on other transient genes were diverse (Figure 3G). Specifically, hox operon and *nifJ* operons have two distinct binding regions at the transcription start sites (TSSs) and middle of operons, *pntAB* operon has two binding regions in the middle and downstream of the operon, and *nrtABCD* operon has one binding region downstream of the operon (Figure 3H). On entry to microoxic conditions, the cyAbrB2 binding signal became less specific as with the general tendency.

Sigma factors SigE and SigA tend to bind cyAbrB2-free promoter regions regardless of GC contents

We searched binding sites of SigE and SigA under aerobic and microoxic conditions (Figures 4A and 4B, top and bottom). Although our peak-calling threshold ignored many minor binding summits, SigE and SigA peaks identified in this study predominantly cover the previously identified peaks (Figure S1D), reproducing the previous study's conclusion (Kariyazono and Osanai, 2022). In other words, SigE and primary sigma factor SigA share localization on the promoters of housekeeping genes, but SigE exclusively binds to the promoters of SigE-dependent genes. SigE and SigA binding signals tend to be weaker in CyAbrB2 binding regions than in CyAbrB2 free regions (Figure 4C). As cyAbrB2 prefers AT-rich regions, we examined whether the peak summits of SigE and SigA are located in regions with high GC contents. Contrary to the expectations, GC contents around peak summits of SigE and SigA were lower compared to that of whole genome (Figure 4D), and no correlation between GC contents and binding signals of SigE and SigA (Figure S3A). When cells enter the microoxic condition, binding signals of both SigA and SigE are changed, although a majority of SigA and SigE peaks in the aerobic condition present in the microoxic condition (Figure 4A).

Next, we focused on Sigma factors dynamics on transiently up-regulated genes. SigE but not SigA binds at TSS of *pntAB* in both aerobic and microoxic conditions. In the aerobic condition, SigE binding summits were not identified at TSSs of hox and nifJ operon. However, SigE-specific binding summit appeared at the TSS of *nifJ* when the cell entered

the microoxic condition (Figure 4E middle). A bimodal peak of SigE appeared at the TSS of *hox* operon, although the peak caller failed to recognize it as two peaks (Figure 4E bottom allow). One side of the bimodal peak near the TSS of hox operon is devoid of SigA binding. Those peaks are consistent with that transiently up-regulated genes which are expressed in a SigE-dependent manner, belong to *hox*, *nifJ*, and *pntAB* operons.

Discussion

The physiological significance of transient upregulation of *hox* and *nifJ* operon

Time course transcriptome revealed that *hox* operon and *nifJ* are transiently up-regulated under the microoxic condition. The reasons for transient upregulation are perhaps the limited number of inorganic cofactors and the reusability of fermentative products. Hydrogenase and NifJ proteins have iron-sulfur clusters, and hydrogenase requires nickel for its activity. A previous study reported that overexpression of hox genes does not achieve a proportional increase in hydrogenase activity without adequate nickel supply (Ortega-Ramos et al., 2014), which suggests continuous expression of *hox* gene is futile in physiological conditions. Furthermore, hydrogen produced by hydrogenase is diffusive and thus difficult to reuse as reducing power when cells return to the aerobic condition. In contrast to hydrogen fermentation, the reverse tricarboxylic acid (rTCA) cycle produces diachronic acids, which are reusable to generate NADPH via the TCA cycle in the aerobic condition. However, adding bicarbonate to phosphoenolpyruvate (PEP) is rate-limiting for rTCA cycle(Hasunuma et al., 2016). Hydrogenase may be advantageous at the initial stage of fermentation because hydrogenase requires only protons for the substrate, and later, the reverse TCA cycle may become active. We classified gene expression of *citH*/*mdh* (sll0891) encoding a key enzyme of reverse TCA cycle as continuously up-regulated genes (Figure 1D).

Significance of multiple regulations of hydrogenase expression

H_2 fermentation is beneficial when the reducing power is in excess, the reverse TCA cycle is less active, and electron acceptors such as oxygen and nitrate are absent. When SigE and cyAbrB2 are working, cells are in the midst of such conditions. In particular, SigE is transcriptionally up-regulated under nitrogen starvation, which means low nitrate condition, and post-transcriptionally activated under dark, meaning the Calvin cycle is inactive (Muro-Pastor et al., 2001; Osanai et al., 2009). SigE transcribes genes catalyzing glycogen catabolism, glycolysis, and oxidative pentose phosphate pathway, and hence produces reducing power. CyAbrB2 and LexA respond to low CO_2, when carboxylation of PEP is slow, and thus reverse TCA is limited. Finally, our result demonstrates that cyAbrB2 responds to low oxygen. Multiple environmental signals are integrated on the *hox* promoter through the dynamics of cyAbrB2, LexA, and SigE.

cyAbrB2 is functionally similar to nucleoid-associated proteins

We have shown that cyAbrB2 broadly binds to AT-rich genomic regions, including insertion element sequences and repress expression (Figures 3B and 3D). This is functionally similar to families of nucleoid-associated proteins; the histone-like nucleoid protein H-NS in Gram-negative bacteria (Fang and Rimsky, 2008; Kahramanoglou et al., 2011) and Lsr2 in Mycobacteria (Gordon et al., 2010). CyAbrB2 binds to hox promoter directly and in a sequence-specific manner (Dutheil et al., 2012), and the present ChIP-seq analysis confirmed in vivo binding to that promoter region. However, ChIP-seq revealed that binding regions of cyAbrB2 are broader than the previously demonstrated region. CyAbrB2 might spread by forming filaments like H-NS. The analogy to H-NS presents a hypothesis that cyAbrB2 bridges genomic regions where cyAbrB2 binds and organizes chromatin conformation and thus globally regulates gene expression.

CyAbrB2 binds gene bodies and/or promoter regions of transiently up-regulated genes and represses them at the aerobic condition, but repression is canceled on entry to the microoxic condition. SigE, LexA, and cyAbrB1 are the candidate of the counter-silencer for cyAbrB2 because the alternative sigma factor, transcription factor, and paralog of

the silencer can be the counter-silencer (Fang and Rimsky, 2008). Alternatively, cyAbrB2 itself could sense the microoxic condition. A previous study reported that cyAbrB2 is glutathionylated in vitro, and glutathionylation affects the binding activity of cyAbrB2 to hox promoter (Sakr et al., 2013). CyAbrB1 shows altered binding efficiency under different redox conditions in vitro (Song et al., 2022).

Insights into transcriptional regulation for hydrogenase expression

SigE and SigA seem to be blocked at the cyAbrB2 bound region (Figure 4C), presumably because sigma factors recognize the promoter as a large complex of RNA polymerase and thus require promoter accessibility. CyAbrB2 binds *hox* promoter region and may inhibit access to the RNA polymerase complex in the aerobic condition. When the cells entry to the microoxic condition, specific binding on hox promoter was less specific, providing space for SigE-containing RNA polymerase. LexA presumably supports SigE binding to *hox* promoter as a lexA binding site is adjacent to the SigE binding site (Figure S3C and 4D, region1). Another binding region in the middle of *hox* operon may be the transcriptional barrier and/or form a chromatin conformation by bridging promoter region and middle of the operon. CyAbrB2 and SigE should exert similar regulation on *nifJ* promoter, presumably in combination with Hik31 and Rre34, a response regulator sensing low oxygen (Summerfield et al., 2011). On the other hand, cyAbrB2 binds the gene body of *pntB* operon and *nrt* operon but not the promoter region, and *pntB* and *nrt* operon are not suppressed by cyAbrB2 under aerobic conditions. This implies an additional regulatory mechanism other than that of *hox* and *nifJ* promoters, such as chromatin conformation change. Actually, (Song et al., 2022) pointed out the possibility that DNA looping inhibits transcription because artificial DNA looping by LacI repressor of *E. coli* can repress cyanobacterial transcription (Camsund et al., 2014).

Roles of cyAbrB2 beyond the regulation of fermentative genes

Previous studies reported that deletion of cyAbrB2 decreased several genes regulated by NtcA, the global

transcriptional regulator of nitrogen metabolism (Ishii and Hihara, 2008) and genes regulated by NdhR and CmpR, the transcriptional regulator of carbon-concentrating mechanism (Orf et al., 2016). CyAbrB2 may support those transcription factors through the modulation of the chromatin conformation.

CyAbrB family is widely conserved in cyanobacteria. A recent study on heterocyst-forming cyanobacteria reported that cyAbrB2 homolog involves in heterocyst differentiation (Higo et al., 2019). CalA, cyAbrB2 homolog in *Anabaena* sp. PCC7120 represses *hetP* and *hepA*, genes required for heterocyst formation. *HetP* and *hepA* are also up-regulated by hetR, the master regulator of heterocyst differentiation. HetR regulates *hetP* and *hepA*, independent of CalA/cyAbrB2, which is analogous to the *hox* gene regulation in *Synechocystis*. Therefore, chromatin conformation mediated by cyAbrB2 might govern various regulations of cyanobacteria ranging from the fermentative gene's transcription to heterocyst differentiation.

EXPERIMENTAL PROCEDURES

Bacterial strain and plasmids

The glucose-tolerant (GT) strain of *Synechocystis* sp. PCC 6803 (Williams, 1988) was used as a wildtype strain in this study. The SigE (sll1689)-disrupted strain (G50) was constructed in a previous study (Osanai et al., 2005). Disruption and epitope-tagging of abrB1(*sll0359*) and abrB2(*sll0822*) were performed by homologous double recombination between the genome and PCR fragment (Williams, 1988). The resulting transformants were selected by three passages on BG-11 plates containing 5 µg/mL kanamycin. Insertion of the epitope tag fragments and gene disruption was confirmed by genomic PCR (Figure S1A). The cyanobacterial strains, oligonucleotides, and plasmids used in this study are listed in Supplemental Table S1, S2 and S3, respectively.

Aerobic and microoxic culture conditions

For aerobic conditions, cells were harvested after cultivation for 24 h in HEPES-buffered BG-11_0 medium (Rippka et al., 1979) buffered with 20 mM HEPES-KOH (pH 7.8) containing 5 mM NH_4Cl under continuous exposure to white light (40 µmol $m^{-2}s^{-1}$) and bubbled with air containing 1% CO_2. (final OD_{730} = 1.4 ~ 1.8). For dark anaerobic culture, the aerobic culture cell was concentrated to OD_{730} 20 with the centrifuge and the resuspension by culture medium. The concentrated cultures were poured into vials, bubbled with N_2 gas and sealed. The sealed vials were shaded and shaken at 30˚C for described times.

Antibodies and immunoblotting

Sample preparation for the immunoblotting was performed as previously described (Kariyazono and Osanai, 2022), and FLAG-tagged proteins were detected by alkaline-phosphatase-conjugated anti-FLAG IgG (A9469, Sigma Aldrich) and 1-Step™ NBT/BCIP substrate solution (Thermo Fisher Scientific).

RNA isolation

Total RNA was isolated with ISOGEN (Nippon gene) according to the manufacturer's instruction and stored at -80˚C until use. We prepared triplicates for each time point for RNA-seq library.

ChIP assay

Two biological replicates were conducted for each ChIP-seq experiment, and one un-tagged control ChIP was done. ChIP and qPCR analyses were conducted as described in a previous study with a few modifications (Kariyazono and Osanai, 2022); FLAG-tagged proteins were immunoprecipitated with FLAG-M2 antibody (F1804 Sigma-Aldrich) conjugated to protein G dynabeads (10003D Invitrogen).

Library preparation and next-generation sequencing

For the ChIP-seq library, input and immunoprecipitated DNA were prepared into multiplexed libraries using either Neb next (E7645 New England Biolabs). For the RNA-seq library, isolated RNA samples were deprived of

ribosomal RNA with Illumina Ribo-Zero Plus rRNA Depletion Kit (20040526 Illumina) and processed into cDNA library for Illumina with NEBNext Ultra II Directional RNA Library Prep Kit for Illumina (E7760 New England Biolabs). Dual index primers were conjugated with NEBNext Multiplex Oligos for Illumina (E6440S New England Biolabs). We pooled all libraries, and the multiplexed libraries were dispatched to Macrogen Japan Inc. and subjected to paired-end sequencing with HiSeqX. Adapter trimming and quality filtering of raw sequence reads were conducted with fastp (Chen et al., 2018) under the default conditions. The paired-end sequences were mapped onto the *Synechocystis* genome (ASM972v1) using Bowtie2 (Langmead and Salzberg, 2012) (ver. 2.4.5 paired-end). Read counts passed fastp and mapped by Bowtie2 are listed in Supplementary Table S4.

RNA-seq analysis

Mapped reads were counted by HT-seq count for the GFF file of ASM972v1, with the reverse strandedness option. EdgeR package (ver. 3.40.1) performed differential expression analysis. Fold change of expression and FDR was used for gene classifying. Fold change of genes expression calculated by edgeR were listed in Supplemental Tables S5, S6, and S7 (time-course of wildtype, *sigE*Δ vs wildtype, and *abrB2*Δ vs wildtype, respectively) .

Genome-wide analyses

Peaks were called with the MACS3 program (ver. 3.0.0b1). For paired-end reads for SigE, SigA, and untagged control ChIP, narrow peaks were called with <1e-20 of the q-value cut-off and ‘--call-summits’ options. Called peak summits from two replicates and untagged control were merged if summits located within 40bp of each other. Peak summits identified in both replicates but not in the control were considered for further analysis. The midpoint of the peak summits for the merged two replicates was further analyzed.

For paired-end reads for cyAbrB2, cyAbrB1, and untagged control ChIP, the broad peak calling methods are done by ‘–broad’ option with <0.05 of the q-value cut-off and <0.05 of the q-value broad cut-off. The intersection of

broad peaks from two replicates excluding the those called by the control was used in subsequent analyses. The positions of the TSS, including internal start sites, were obtained from a previous study (Kopf et al., 2014). The read count, merging and intersection of the binding region were calculated using BEDTools (ver. 2.30.0) (Quinlan and Hall, 2010). The peaks of SigA and SigE and the broad binding region of cyAbrB2 and cyAbrB1 are listed in Supplemental Tables S8 to S14, respectively.

Binding signals in every 100bp bin for scatter plots were calculated as (IP read counts within 100bp window) / (Input read counts within 100bp window) * (total Input read counts/total IP read counts). GC contents were calculated within 500bp in 100bp sliding windows by seqkit (ver. 2.3.0) (Shen et al., 2016).

Statistical analysis

Statistical analyses were performed with R version 4.2.2. ‘fisher.test’ function performed Fisher’s exact test, and p-values less than 0.05 were denoted as asterisks in the figure. Multiple comparisons of Fisher's exact test were performed by ‘Fisher. multcomp’ function in the RVAideMemoire package. P-values were adjusted by ‘fdr’ method, and FDRs less than 0.05 were shown in the figures. Multiple comparisons of Wilcoxon rank test were performed by ‘pairwise.wilcox.test’, and p-values were adjusted by the ‘fdr’ method. Adjusted p-values less than 0.05 are shown in the figure. Correlation coefficient was calculated with ‘cor’ function.

ACCESSION NUMBERS

Raw ChIP sequencing and RNA sequencing reads were deposited in the Sequence Read Archive (accession ID: PRJNA956842).

Acknowledgments

This study was supported by the following grants to T.O.: Grant-in-Aid for Scientific Research (B) (grant no. 20H02905) and JST-ALCA of the Japan Science and Technology Agency (grant number JPMJAL1306). We thank

Dr. Kohki Yoshimoto for providing laboratory instruments, and Ms. Kaori Iwazumi for the support of bacterial culture and the medium preparation.

Conflicts of interest

There are no conflicts of interest to declare.

Author contributions

RK and TO designed the study; RK performed the experiment; RK analyzed the data; RK and TO wrote the paper.

References

Appel, J., Phunpruch, S., Steinmüller, K., and Schulz, R. (2000). The bidirectional hydrogenase of Synechocystis sp. PCC 6803 works as an electron valve during photosynthesis. Arch. Microbiol. *173*, 333–338.

Camsund, D., Heidorn, T., and Lindblad, P. (2014). Design and analysis of LacI-repressed promoters and DNA-looping in a cyanobacterium. J. Biol. Eng. *8*, 4.

Carrieri, D., Wawrousek, K., Eckert, C., Yu, J., and Maness, P.-C. (2011). The role of the bidirectional hydrogenase in cyanobacteria. Bioresour. Technol. *102*, 8368–8377.

Cassier-Chauvat, C., Veaudor, T., and Chauvat, F. (2014). Advances in the function and regulation of hydrogenase in the cyanobacterium Synechocystis PCC6803. Int. J. Mol. Sci. *15*, 19938–19951.

Chen, S., Zhou, Y., Chen, Y., and Gu, J. (2018). fastp: an ultra-fast all-in-one FASTQ preprocessor. Bioinformatics *34*, i884–i890.

Dutheil, J., Saenkham, P., Sakr, S., Leplat, C., Ortega-Ramos, M., Bottin, H., Cournac, L., Cassier-Chauvat, C., and Chauvat, F. (2012). The AbrB2 autorepressor, expressed from an atypical promoter, represses the hydrogenase operon to regulate

hydrogen production in Synechocystis strain PCC6803. J. Bacteriol. *194*, 5423–5433.

Fang, F.C., and Rimsky, S. (2008). New insights into transcriptional regulation by H-NS. Curr. Opin. Microbiol. *11*, 113–120.

Gordon, B.R.G., Li, Y., Wang, L., Sintsova, A., van Bakel, H., Tian, S., Navarre, W.W., Xia, B., and Liu, J. (2010). Lsr2 is a nucleoid-associated protein that targets AT-rich sequences and virulence genes in Mycobacterium tuberculosis. Proc. Natl. Acad. Sci. *107*, 5154–5159.

Gutekunst, K., Phunpruch, S., Schwarz, C., Schuchardt, S., Schulz-Friedrich, R., and Appel, J. (2005). LexA regulates the bidirectional hydrogenase in the cyanobacterium Synechocystis sp. PCC 6803 as a transcription activator. Mol. Microbiol. *58*, 810–823.

Gutekunst, K., Chen, X., Schreiber, K., Kaspar, U., Makam, S., and Appel, J. (2014). The bidirectional NiFe-hydrogenase in Synechocystis sp. PCC 6803 is reduced by flavodoxin and ferredoxin and is essential under mixotrophic, nitrate-limiting conditions. J. Biol. Chem. *289*, 1930–1937.

Hasunuma, T., Matsuda, M., and Kondo, A. (2016). Improved sugar-free succinate production by Synechocystis sp. PCC 6803 following identification of the limiting steps in glycogen catabolism. Metab. Eng. Commun. *3*, 130–141.

Higo, A., Nishiyama, E., Nakamura, K., Hihara, Y., and Ehira, S. (2019). cyAbrB Transcriptional Regulators as Safety Devices To Inhibit Heterocyst Differentiation in Anabaena sp. Strain PCC 7120. J. Bacteriol. *201*.

Iijima, H., Shirai, T., Okamoto, M., Pinto, F., Tamagnini, P., Hasunuma, T., Kondo, A., Hirai, M.Y., and Osanai, T. (2016). Metabolomics-based analysis revealing the alteration of primary carbon metabolism by the genetic manipulation of a hydrogenase HoxH in Synechocystis sp. PCC 6803. Algal Res. *18*, 305–313.

Iijima, H., Watanabe, A., Sukigara, H., Iwazumi, K., Shirai, T., Kondo, A., and Osanai, T. (2021). Four-carbon dicarboxylic acid production through the reductive branch of the open cyanobacterial tricarboxylic acid cycle in Synechocystis sp. PCC 6803. Metab. Eng. *65*, 88–98.

Imamura, S., and Asayama, M. (2009). Sigma factors for cyanobacterial transcription. Gene Regul. Syst. Bio. *3*, 65–87.

Ishii, A., and Hihara, Y. (2008). An AbrB-like transcriptional regulator, Sll0822, is essential for the activation of nitrogen-regulated genes in Synechocystis sp. PCC 6803. Plant Physiol. *148*, 660–670.

Kahramanoglou, C., Seshasayee, A.S.N., Prieto, A.I., Ibberson, D., Schmidt, S., Zimmermann, J., Benes, V., Fraser, G.M., and Luscombe, N.M. (2011). Direct and indirect effects of H-NS and Fis on global gene expression control in Escherichia coli. Nucleic Acids Res. *39*, 2073–2091.

Kariyazono, R., and Osanai, T. (2022). Identification of the genome-wide distribution of cyanobacterial group-2 sigma factor SigE, accountable for its regulon. Plant J. *110*, 548–561.

Kopf, M., Klähn, S., Pade, N., Weingärtner, C., Hagemann, M., Voß, B., and Hess, W.R. (2014). Comparative genome analysis of the closely related Synechocystis strains PCC 6714 and PCC 6803. DNA Res. *21*, 255–266.

Langmead, B., and Salzberg, S.L. (2012). Fast gapped-read alignment with Bowtie 2. Nat. Methods *9*, 357–359.

Leplat, C., Champeimont, R., Saenkham, P., Cassier-Chauvat, C., Jean-Christophe, A., and Chauvat, F. (2013). Genome-wide transcriptome analysis of hydrogen production in the cyanobacterium Synechocystis: Towards the identification of new players. Int. J. Hydrogen Energy *38*, 1866–1872.

Lieman-Hurwitz, J., Haimovich, M., Shalev-Malul, G., Ishii, A., Hihara, Y., Gaathon, A., Lebendiker, M., and Kaplan, A. (2009). A cyanobacterial AbrB-like protein affects the apparent photosynthetic affinity for CO2 by modulating low-CO2-induced gene expression. Environ. Microbiol. *11*, 927–936.

McNeely, K., Xu, Y., Bennette, N., Bryant, D.A., and Dismukes, G.C. (2010). Redirecting reductant flux into hydrogen production via metabolic engineering of fermentative carbon metabolism in a cyanobacterium. Appl. Environ. Microbiol. *76*, 5032–5038.

Muro-Pastor, A.M., Herrero, A., and Flores, E. (2001). Nitrogen-regulated group 2 sigma factor from Synechocystis sp. strain

PCC 6803 involved in survival under nitrogen stress. J. Bacteriol. *183*, 1090–1095.

Oliveira, P., and Lindblad, P. (2005). LexA, a transcription regulator binding in the promoter region of the bidirectional hydrogenase in the cyanobacterium Synechocystis sp. PCC 6803. FEMS Microbiol. Lett. *251*, 59–66.

Oliveira, P., and Lindblad, P. (2008). An AbrB-Like protein regulates the expression of the bidirectional hydrogenase in Synechocystis sp. strain PCC 6803. J. Bacteriol. *190*, 1011–1019.

Orf, I., Schwarz, D., Kaplan, A., Kopka, J., Hess, W.R., Hagemann, M., and Klähn, S. (2016). CyAbrB2 Contributes to the Transcriptional Regulation of Low CO2 Acclimation in Synechocystis sp. PCC 6803. Plant Cell Physiol. *57*, 2232–2243.

Ortega-Ramos, M., Jittawuttipoka, T., Saenkham, P., Czarnecka-Kwasiborski, A., Bottin, H., Cassier-Chauvat, C., and Chauvat, F. (2014). Engineering Synechocystis PCC6803 for hydrogen production: influence on the tolerance to oxidative and sugar stresses. PLoS One *9*, e89372.

Osanai, T., Kanesaki, Y., Nakano, T., Takahashi, H., Asayama, M., Shirai, M., Kanehisa, M., Suzuki, I., Murata, N., and Tanaka, K. (2005). Positive regulation of sugar catabolic pathways in the cyanobacterium Synechocystis sp. PCC 6803 by the group 2 sigma factor sigE. J. Biol. Chem. *280*, 30653–30659.

Osanai, T., Imashimizu, M., Seki, A., Sato, S., Tabata, S., Imamura, S., Asayama, M., Ikeuchi, M., and Tanaka, K. (2009). ChlH, the H subunit of the Mg-chelatase, is an anti-sigma factor for SigE in Synechocystis sp. PCC 6803. Proc. Natl. Acad. Sci. U. S. A. *106*, 6860–6865.

Osanai, T., Oikawa, A., Azuma, M., Tanaka, K., Saito, K., Hirai, M.Y., and Ikeuchi, M. (2011). Genetic engineering of group 2 sigma factor SigE widely activates expressions of sugar catabolic genes in Synechocystis species PCC 6803. J. Biol. Chem. *286*, 30962–30971.

Osanai, T., Shirai, T., Iijima, H., Nakaya, Y., Okamoto, M., Kondo, A., and Hirai, M.Y. (2015). Genetic manipulation of a metabolic enzyme and a transcriptional regulator increasing succinate excretion from unicellular cyanobacterium . Front.

Microbiol. *6*, 1064.

Puggioni, V., Tempel, S., and Latifi, A. (2016). Distribution of Hydrogenases in Cyanobacteria: A Phylum-Wide Genomic Survey. Front. Genet. *7*, 223.

Quinlan, A.R., and Hall, I.M. (2010). BEDTools: a flexible suite of utilities for comparing genomic features. Bioinformatics *26*, 841–842.

Rippka, R., Deruelles, J., and Waterbury, J.B. (1979). Generic assignments, strain histories and properties of pure cultures of cyanobacteria. J. Gen. Microbiol. *111*, 1–61.

Sakr, S., Dutheil, J., Saenkham, P., Bottin, H., Leplat, C., Ortega-Ramos, M., Aude, J.-C., Chapuis, V., Guedeney, G., Decottignies, P., et al. (2013). The activity of the Synechocystis PCC6803 AbrB2 regulator of hydrogen production can be post-translationally controlled through glutathionylation. Int. J. Hydrogen Energy *38*, 13547–13555.

Shen, W., Le, S., Li, Y., and Hu, F. (2016). SeqKit: A Cross-Platform and Ultrafast Toolkit for FASTA/Q File Manipulation. PLoS One *11*, e0163962.

Song, K., Hagemann, M., Georg, J., Maaß, S., Becher, D., and Hess, W.R. (2022). Expression of the Cyanobacterial F(o)F(1) ATP Synthase Regulator AtpΘ Depends on Small DNA-Binding Proteins and Differential mRNA Stability. Microbiol. Spectr. *10*, e0256221.

Stal, L.J., and Moezelaar, R. (1997). Fermentation in cyanobacteria1Publication 2274 of the Centre of Estuarine and Coastal Ecology, Yerseke, The Netherlands.1. FEMS Microbiol. Rev. *21*, 179–211.

Summerfield, T.C., Nagarajan, S., and Sherman, L.A. (2011). Gene expression under low-oxygen conditions in the cyanobacterium Synechocystis sp. PCC 6803 demonstrates Hik31-dependent and -independent responses. Microbiology *157*, 301–312.

Williams, J.G.K. (1988). Construction of Specific Mutations in Photosystem II Photosynthetic Reaction Center by Genetic

Engineering Methods in Synechocystis 6803. In Methods in Enzymology, (Academic Press), pp. 766–778.

Yamauchi, Y., Kaniya, Y., Kaneko, Y., and Hihara, Y. (2011). Physiological roles of the cyAbrB transcriptional regulator pair Sll0822 and Sll0359 in Synechocystis sp. strain PCC 6803. J. Bacteriol. *193*, 3702–3709.

Table 1 List of transiently upregulated genes

		Operon [a]
Oxidoreductase		
sll0741	nifJ/"pyruvate-ferredoxin/flavodoxin oxidoreductase"	
sll0743	hypothetical protein	TU3296
sll0744	dihydroorotate dehydrogenase (fumarate)	
sll1221	**hoxF/"bidirectional [NiFe] hydrogenase diaphorase subunit"**	
sll1222	**unknown protein**	
sll1223	**hoxU/"bidirectional [NiFe] hydrogenase diaphorase subunit"**	**TU1714**
sll1224	**hoxY/"NAD-reducing hydrogenase small subunit"**	
sll1225	**unknown protein**	
sll1226	**hoxH/"NAD-reducing hydrogenase large subunit"**	
slr1434	pntB/"H^+-translocating NAD(P) transhydrogenase subunit beta"	TU1089
Transporter		
sll1450	**nrtA/"nitrate/nitrite transport system substrate-binding protein"**	
sll1451	**nrtB/"nitrate/nitrite transport system permease protein"**	**TU1023**
sll1452	**nrtC/"nitrate/nitrite transport system ATP-binding protein"**	
sll1453	**nrtD/"nitrate/nitrite transport system ATP-binding protein"**	
Two-component system		
slr1214	twitching motility two-component system response regulator PilG	TU905
slr1215	**unknown protein**	**TU907**
Glycosyl transferase		
slr2116	spsA/"spore coat polysaccharide biosynthesis protein; SpsA"	TU1673
Protease		
sll1009	**frpC/"iron-regulated protein"**	**TU491**
Transposase		
slr1523	transposase	TU1659
sll1985	**transposase**	**TU1589**
sll7001	transposase	NA
sll7003	toxin FitB	TU7001
ssl0172	transposase	TU3163
Other		
slr1260	hypothetical protein	TU1446
slr0668	unknown protein	TU3532
slr5127	unknown protein	TU5127
sll0710	unknown protein	TU97
sll1307	unknown protein	TU1224

The list of transiently upregulated genes is merged by transcriptional units and sorted by function. The transcriptional unit information is from the previous study (Kopf et al., 2014).

Figure 1

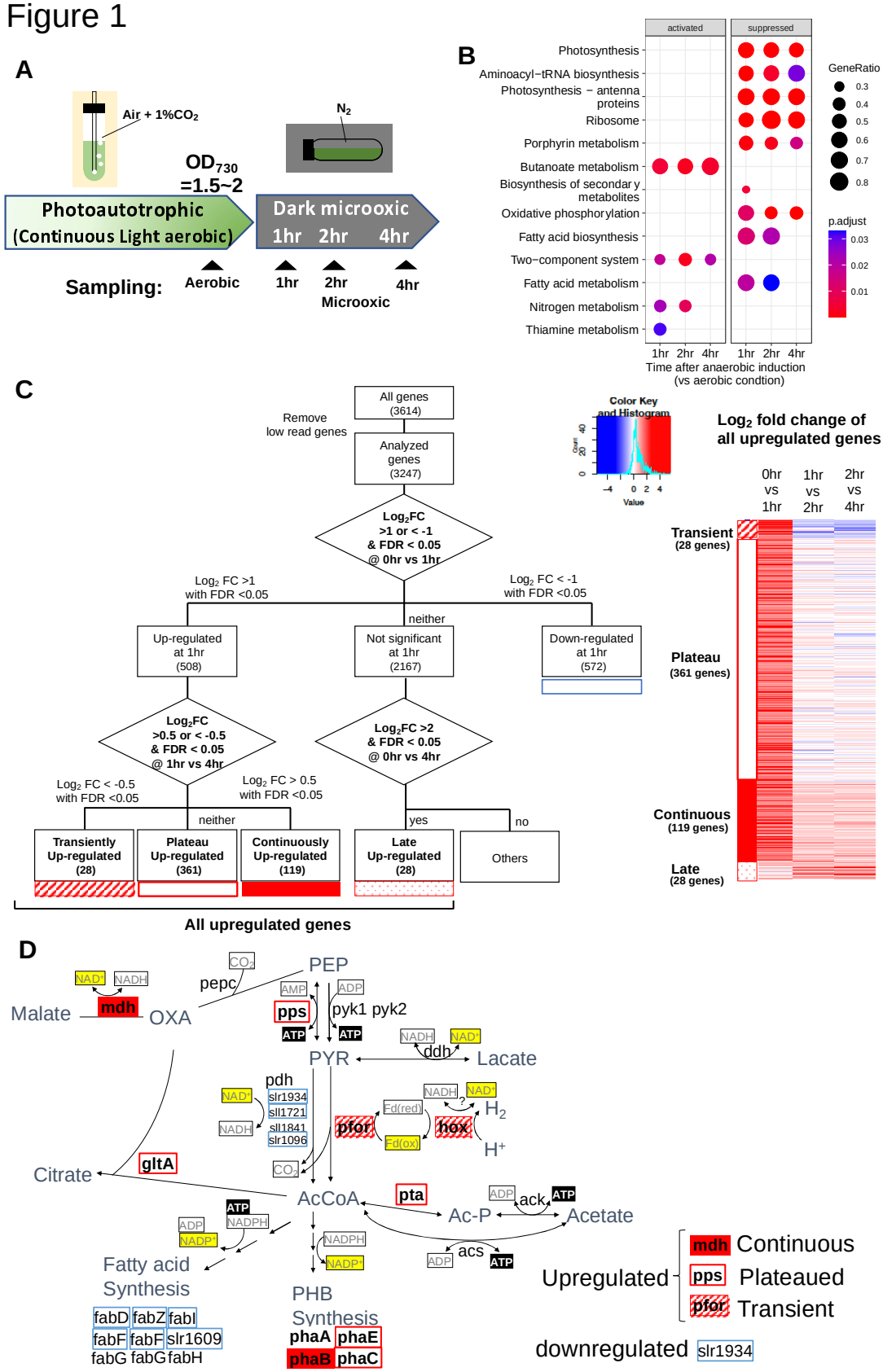

Figure 1

(A) Schematic diagram for the sampling of cells under aerobic and microoxic conditions. (B) Gene set enrichment

analysis on time-course transcriptome data. KEGG pathways enriched in up-regulated or downregulated genes after 1hr, 2hr, and 4hr incubation in the anaerobic condition are shown. (C) (left) Schematic diagram showing the classification of genes according to the time-course transcriptome. Transient (striped square), Plateau (open square), Continuous (filled square), and Late (dotty square) are denoted as all up-regulated genes. (right) Heatmap showing expression change of all up-regulated genes over the time-course. Genes are clustered in subgroups and sorted by the gene name. (D) The classified genes mapped to the central carbon metabolism, centered by pyruvate. The abbreviation of compounds; PEP: phosphoenolpyruvate, PYR: pyruvate, AcCoA: acetyl CoA, Ac-P: acetyl phosphate, OXA: oxaloacetate, PHB: polyhydroxy butyrate.

Figure 2

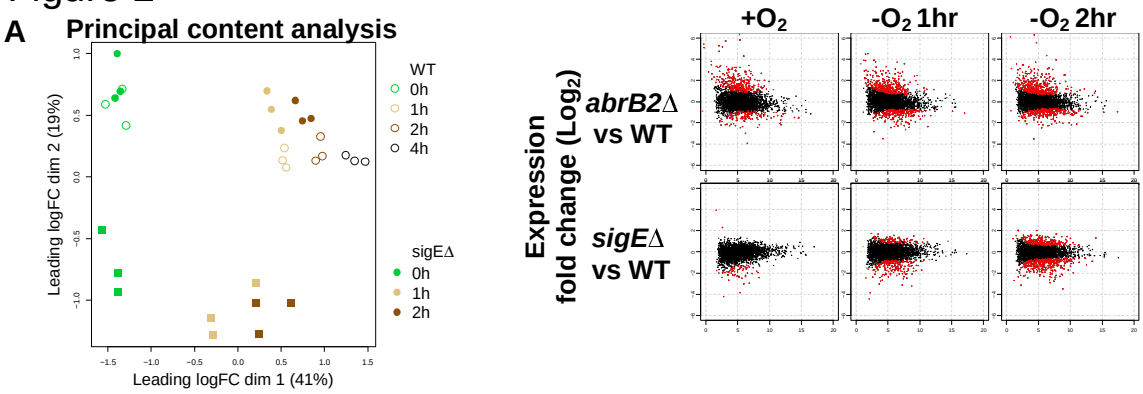

B

hox operon

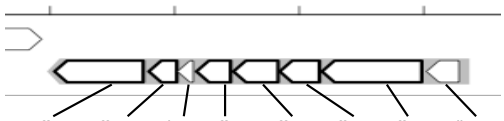

		sll1226 hoxH	sll1225 hoxY	ssl2420	sll1224	sll1223 hoxU	sll1222	sll1221 hoxF	sll1220 hoxE
abrB2Δ vs WT	0hr	+1.75	+0.18	+1.05	+1.42	+1.58	+0.69	+1.13	+0.79
	1hr	-1.62	-2.00	-1.27	-0.57	-0.25	-0.45	-0.27	-0.27
	2hr	-0.82	-0.55	-0.13	-0.02	+0.19	+0.2	+0.3	+0.23
sigEΔ vs WT	0hr	-0.24	-0.01	-0.14	-0.41	-0.52	-0.78	-0.66	-1.31
	1hr	-1.45	-1.59	-1.56	-1.01	-1.59	-1.61	-2.07	-2.35
	2hr	-1.45	-1.41	-1.64	-1.34	-1.92	-1.71	-2.43	-2.91

nifJ operon

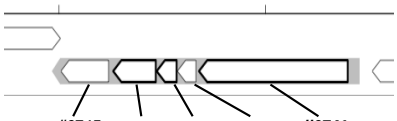

		sll0745 pfkA	sll0744	sll0743	sll0742	sll0741 nifJ
abrB2Δ vs WT	0hr	NA	+1.65	0.02	+0.62	+0.86
	1hr	NA	-0.60	-1.05	-0.11	+0.25
	2hr	NA	+0.11	-0.16	+0.68	+0.79
sigEΔ vs WT	0hr	NA	-0.89	-0.81	-0.49	-1.59
	1hr	NA	-1.73	-2.07	-1.62	-2.09
	2hr	NA	-1.71	-1.96	-1.52	-2.31

Expression fold change (Log_2)

C

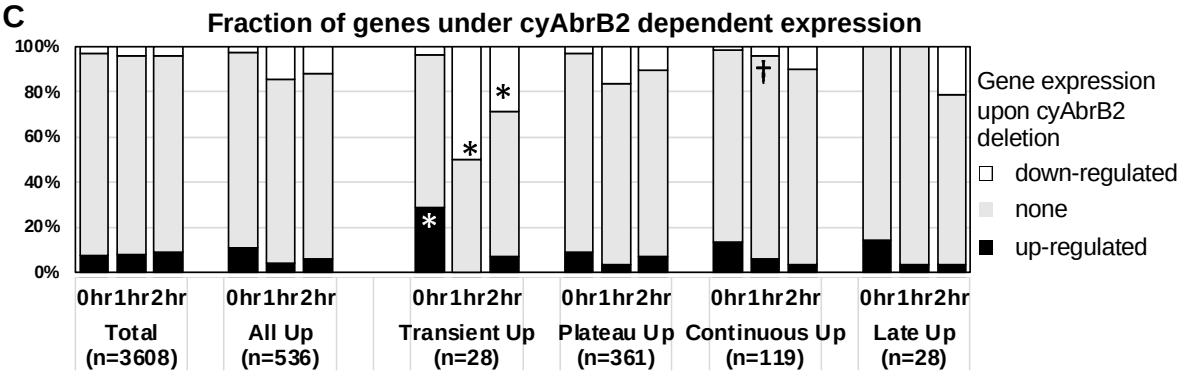

D

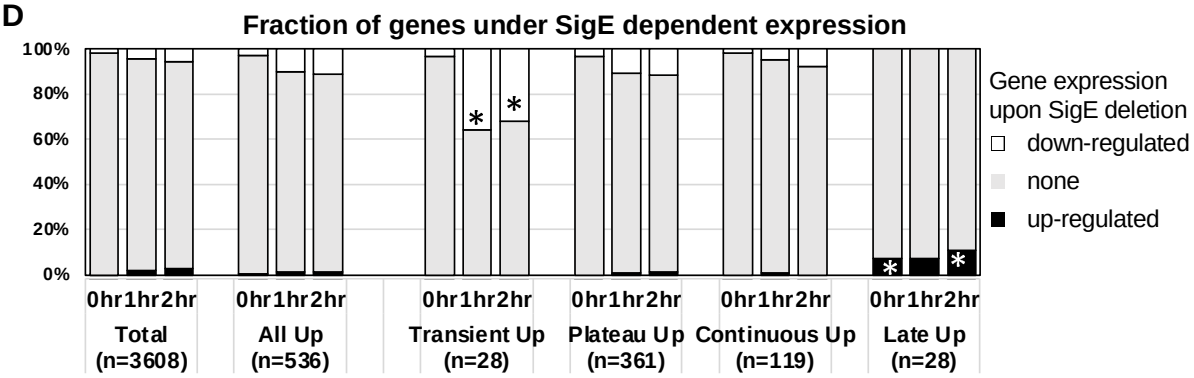

Figure 2

(A) (left) Primary component scatter plot showing the profiles of RNA-seq data. (right) MA plot showing fold change (y

axis) and average (x axis) of gene expression between wild type and mutant strains at each time point. Red dots indicates defined DEGs ($|Log_2 FC| > 1$ with FDR < 0.05) (B) Log2 scaled expression fold change of genes in *hox* operon and *nifJ* operon upon the deletion of cyAbrB2 and SigE under the aerobic condition (0hr), 1hr after anoxic condition (1hr), and 2hr after anoxic condition (2hr). DEGs are marked with sky blue (down-regulated upon deletion) or red (up-regulated upon deletion). (C and D) Fraction of up-regulated and down-regulated genes upon the deletion of (C) cyAbrB2 and (D)SigE at the time points of the aerobic condition (0hr), 1hr after anoxic condition (1hr), and 2hr after anoxic condition (2hr). Genes are classified according to Figure 1C. Asterisk (*) and dagger (†) denote statistically significant enrichment and anti-enrichment compared with all up-regulated genes tested by multiple comparisons of Fisher's exact test (FDR < 0.05).

Figure 3

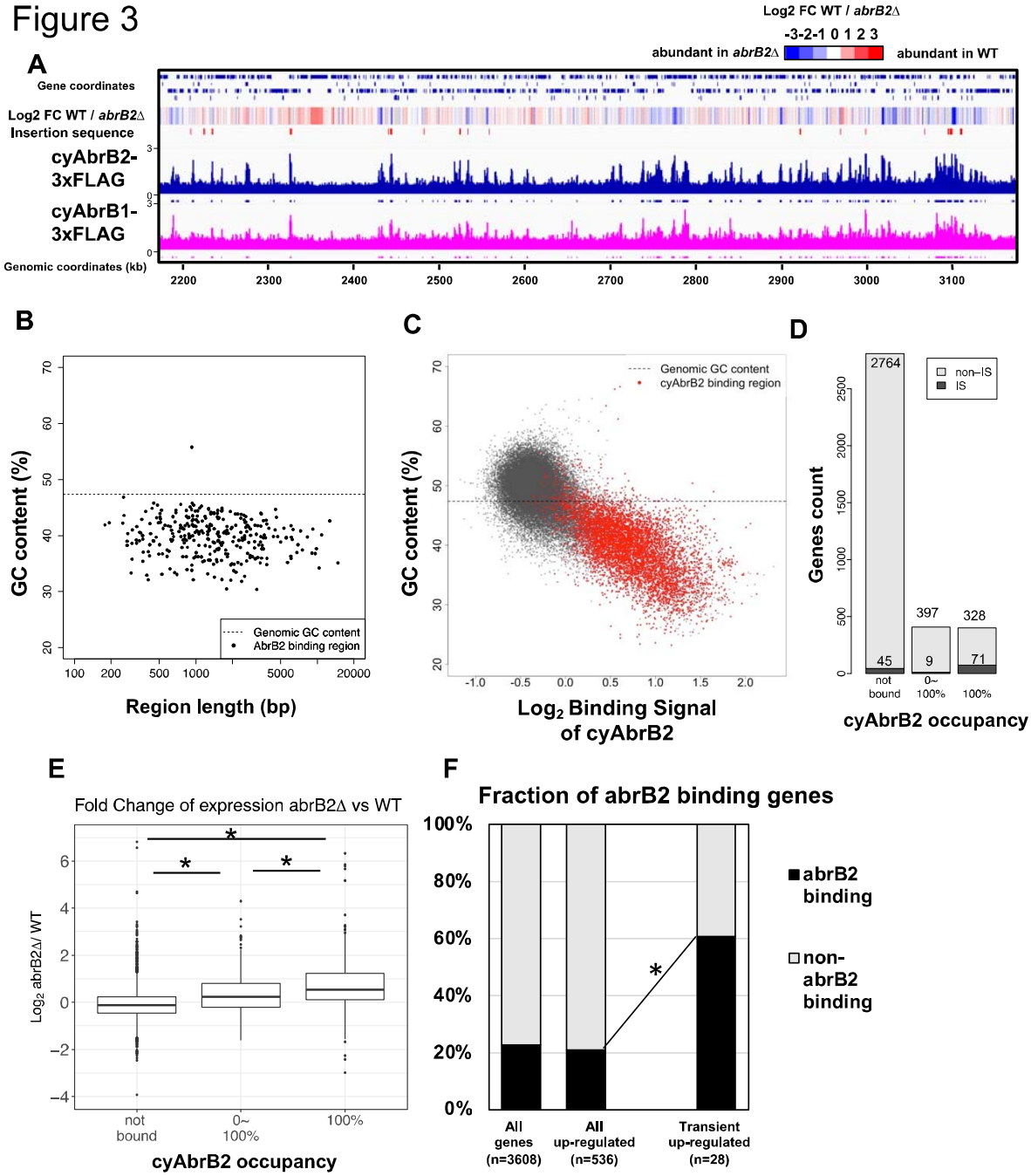

Figure3 (continuing)

Figure3 (continued)

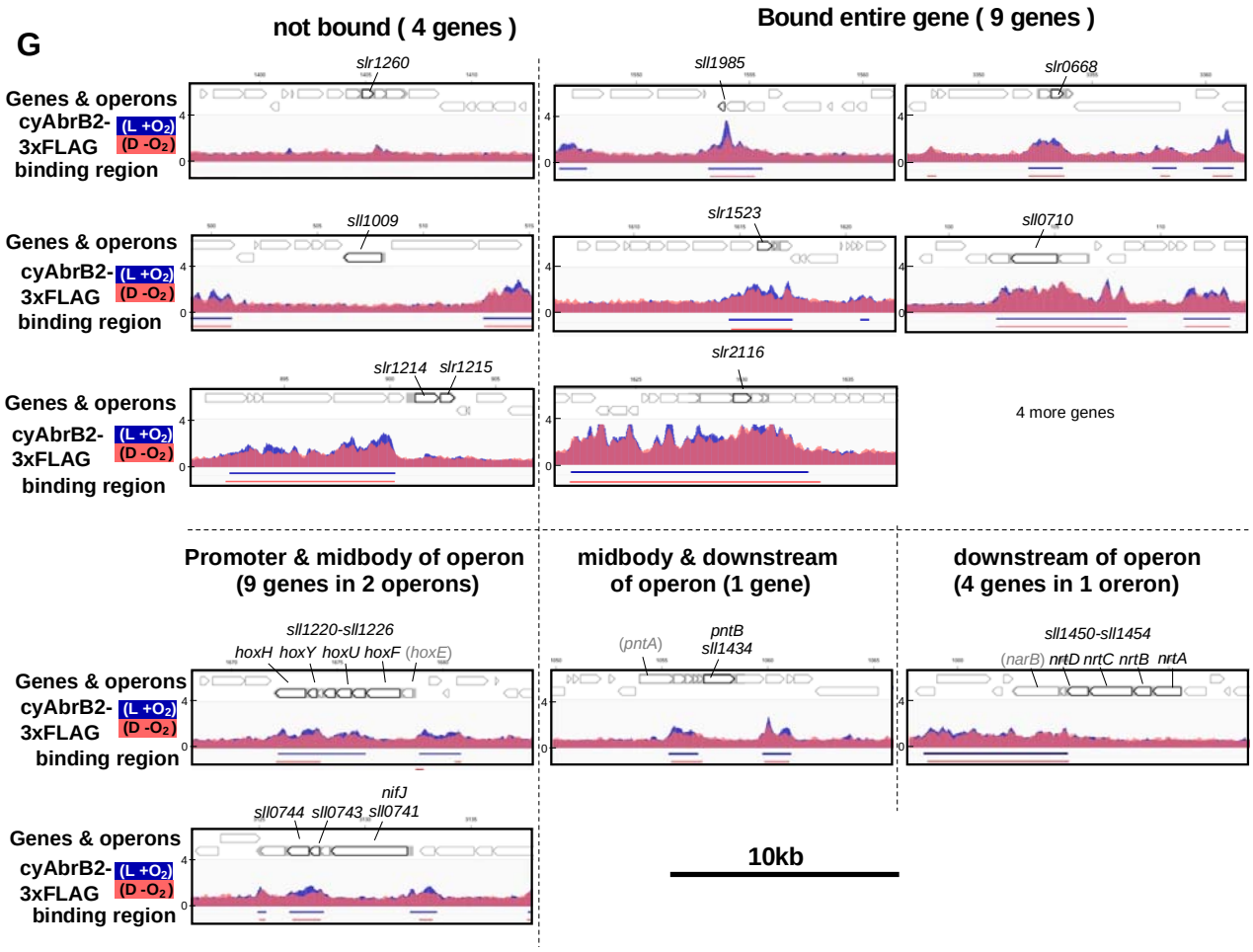

Figure 3

(A) The snapshot of ChIP-seq data for cyAbrB2 and cyAbrB1 in the aerobic condition. The heatmap in the second column indicates expression fold change upon cyAbrB2 deletion at the aerobic condition. Positive values (colored in red) indicate the gene expression is higher in wildtype than *cyabrB2*Δ, and negative values (colored in blue) indicate the gene expression is higher in *cyabrB2*Δ than in wildtype. The third column indicates positions for the insertion elements.

(B) GC contents and region length of cyAbrB2 binding regions (black dots). The horizontal dotty line indicates the genomic average of GC content.

(C) Scatter plot of GC content and binding signal of cyAbrB2. The X-axis is the binding signal of cyAbrB2 in each 100bp region, and the Y-axis indicates GC contents within 500bp windows sliding every 100 base pairs.

(D)Histogram of genes showing the extent of occupancy (not bound, partially overlapped, entirely overlapped) by cyAbrB2 binding region. The gray bars indicate non-IS genes and count numbers of non-IS genes are displayed on the gray bars. The black bars indicate IS genes and count numbers of IS genes are displayed on the black bars.

(E) Boxplot showing fold change of gene expression by abrB2 deletion under the aerobic condition. Genes are classified according to the extent of occupancy by cyAbrB2 binding region.

(F) Fraction of genes overlapped or non-overlapped with cyAbrB2 binding regions at the time points of the aerobic condition. Genes are classified according to Figure 1C. Asterisk (*) denotes statistically significant enrichment compared with all up-regulated genes tested by multiple comparisons of Fisher's exact test.

(G) Distribution of cyAbrB2 around transiently up-regulated genes. ChIP-seq data in aerobic (L $+O_2$) and dark microoxic (D $-O_2$) conditions are overlayed. Arrows with bold lines indicate transiently up-regulated genes. Shaded arrows indicate operons whose data is from the previous study. The bars below the graph indicate the binding regions of each protein. The black bar top of the figure indicates a length of 10kbp.

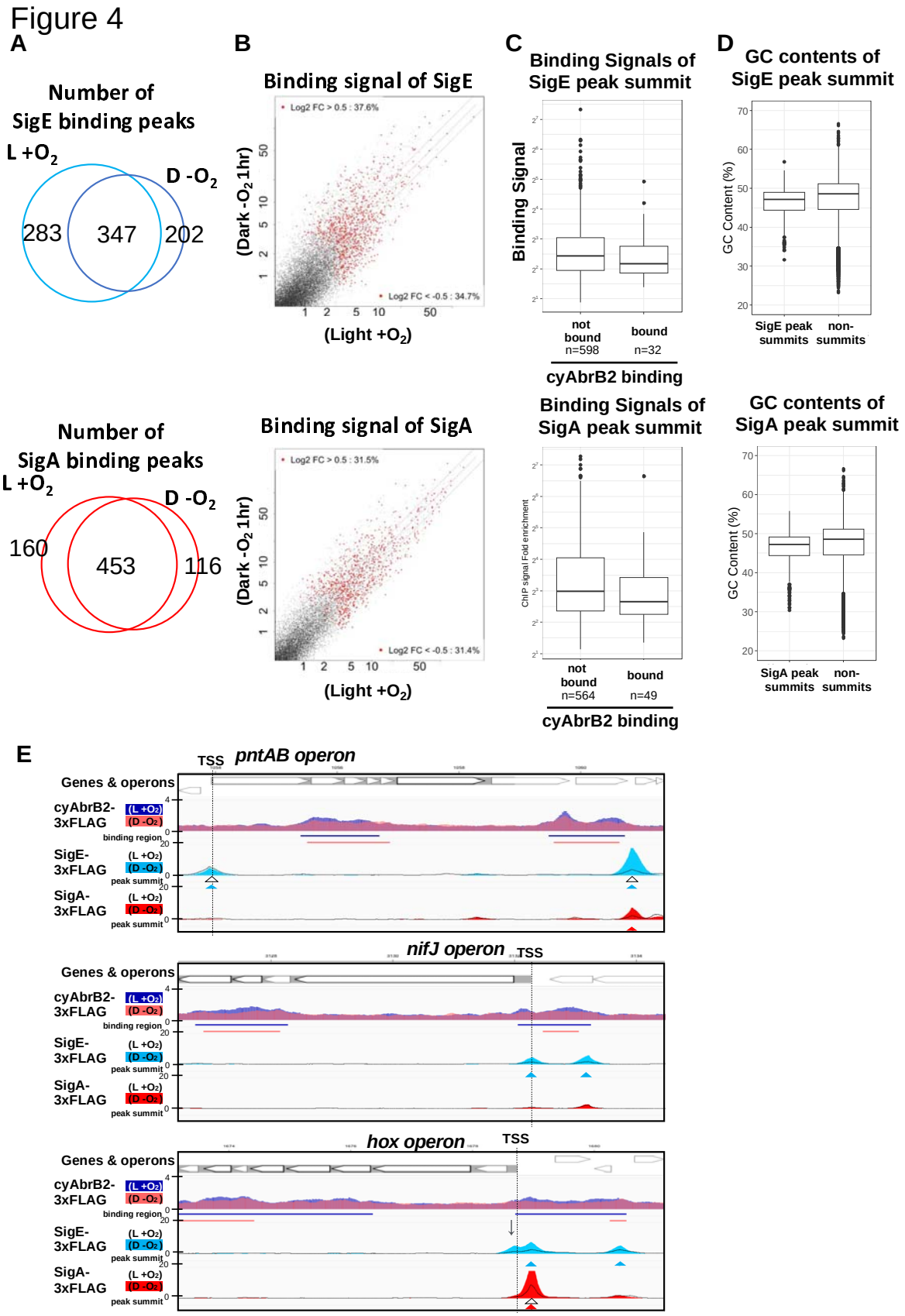

Figure 4

(A) Venn diagram showing the number of peaks of SigE and SigA in aerobic (L + O_2) and dark microoxic (D -O_2)

conditions. (B) Scatter plot showing changes of the binding signal of SigE and SigA by 1hr cultivation in the microoxic condition. The binding signal of each 100bp window is plotted. The binding signals are plotted as Figure 3E. (C) Distribution of ChIP enrichment signals of SigE and SigA peaks. Peaks are binary classified by whether peaks are located in the cyAbrB2-binding region. (D) (E) Snapshots of ChIP-seq data for abrB2, SigE, and SigA at *nifJ* region (top) and *hox* region (bottom). ChIP-seq data of cyAbrB2, SigE, and SigA in aerobic and dark microoxic conditions are overlayed. ChIP-seq data of cyAbrB2 in aerobic and microoxic conditions are colored blue and pink, respectively. ChIP-seq data of SigE and SigA are shown in solid lines (aerobic conditions) and filled lines (microoxic conditions). Positions of TSSs are from the previous study (Kopf et al., 2014) and indicated by vertical dotted lines. Open triangles indicate peak summits under the aerobic condition, and solid triangles indicate peak summits under the microoxic condition.

Figure 5

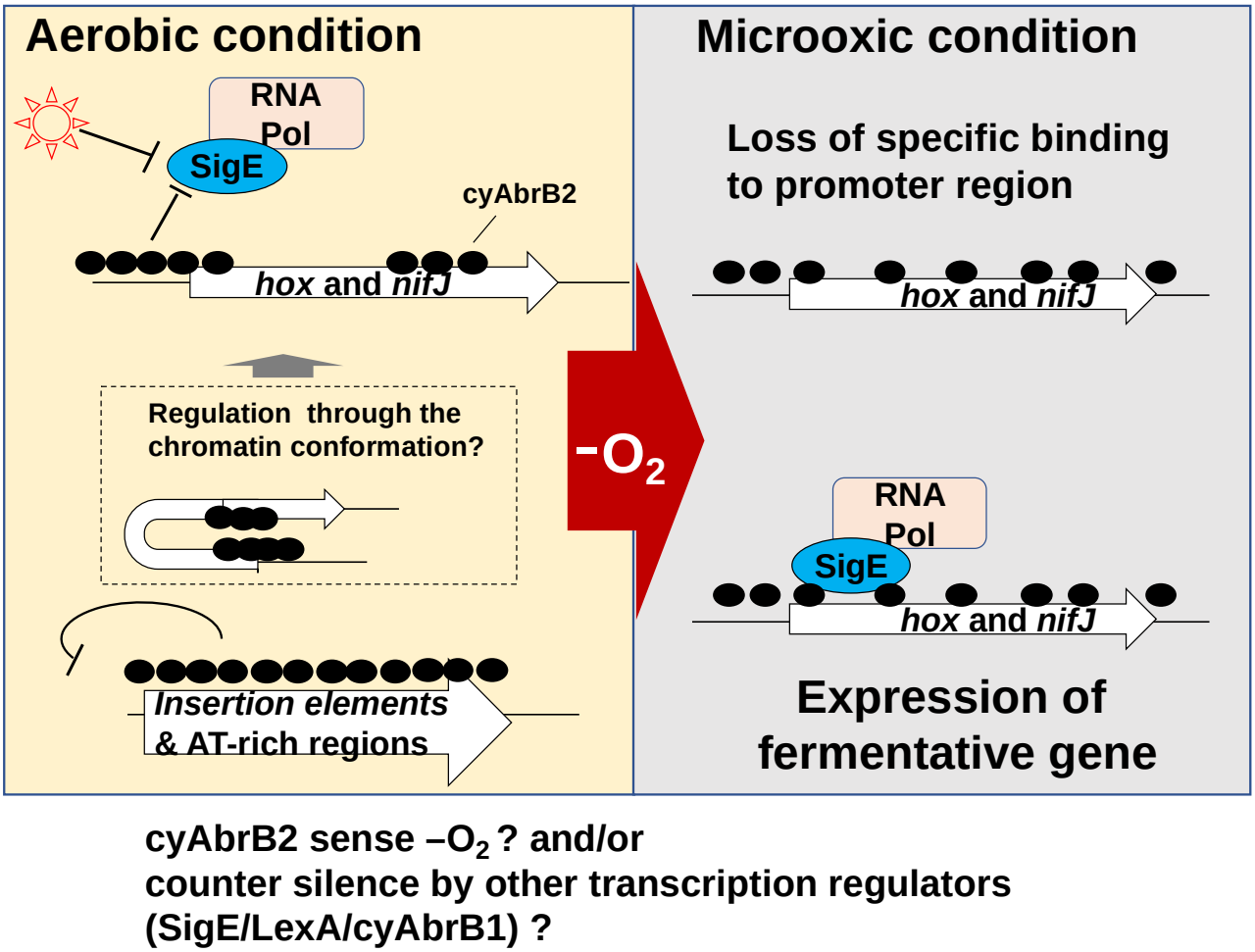

Figure 5

The schematic diagram for the dynamics of transcription factors governing the expression of fermentative genes.

Figure S1

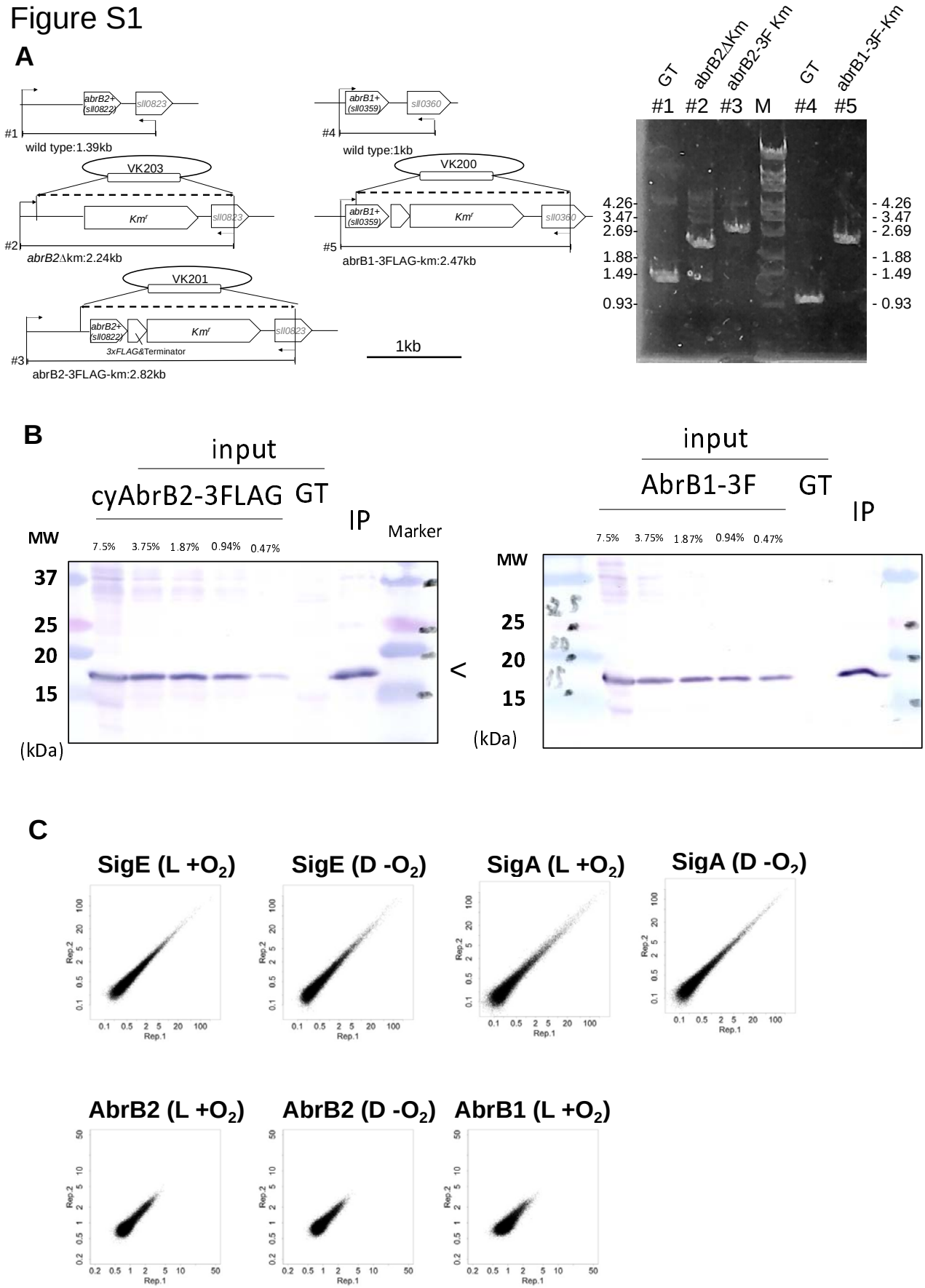

Figure S1 (continuing)

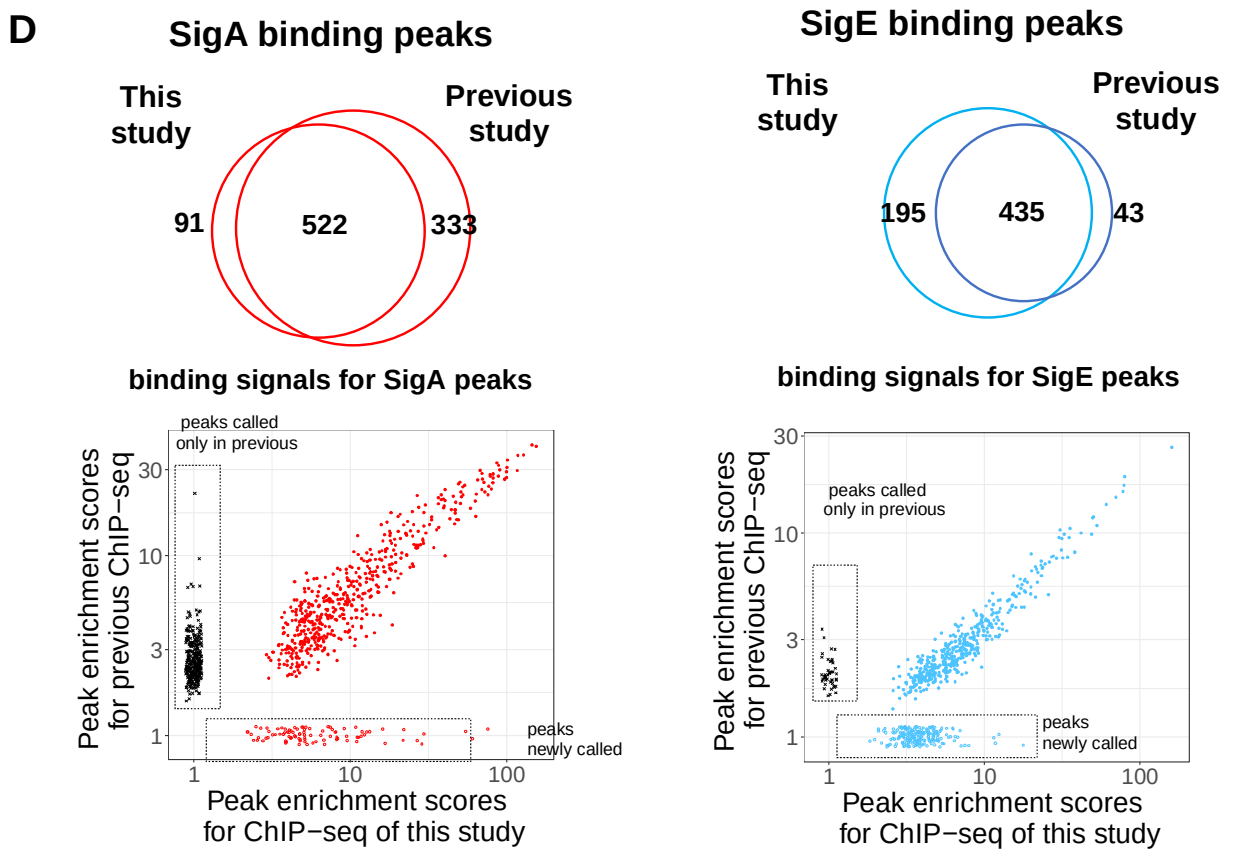

Figure S1

Validation of procedure for ChIP-seq of flag tagged cyAbrB2, SigE, and SigA.

(A) Confirmation of genomic deletion and the epitope tagging of abrB2 (#1-#3) and the epitope tagging of abrB1 (#4 and #5). (B) The immunoblot for inputs and immunoprecipitants of ChIP for cyAbrB2-FLAG and cyAbrB1-FLAG. Inputs equivalent to indicated portion of IP were loaded. (C)Scatter plots showing reproducibility of two replicates for ChIP-seq assay. ChIP-seq data of SigE, SigA, and cyAbrB2 in aerobic and microoxic conditions and ChIP-seq data of cyAbrB1 in the aerobic condition are shown. Dots indicates normalized IP read count / normalized input read count in each 100bp windows. X axis is value of replicate1 and Y axis is value of replicate 2. (D) Reproducibility of ChIP-seq data of SigA and SigE, compared with the previous study (Kariyazono and Osanai 2022). (top) Pie charts show overlapping of peaks called in this studies and the previous study. (bottom) Scatter plot comparing ChIP binding signals of SigA and SigE peaks commonly called in present and previous studies. Plots boxed by dashed line are peaks called only in present or previous study.

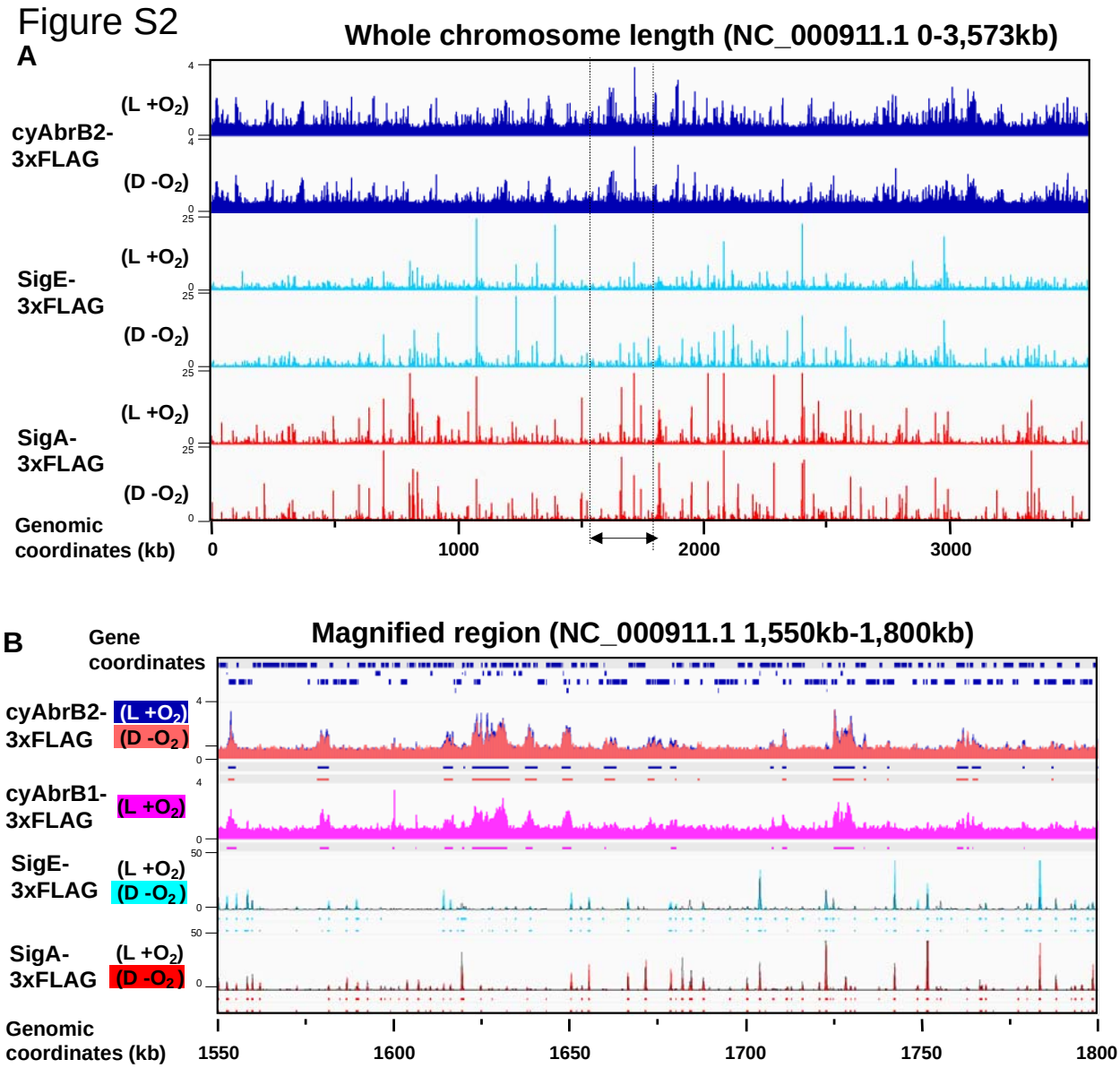

Figure S2

Overview for ChIp-seq of flag tagged cyAbrB2,cyAbrB1, SigE, and SigA. Y-axis indicates [normalized IP read count / normalized input read count at each 25bp window] and X- axis indicates chromosome position.

(A) Distribution of cyAbrB2, cyAbrB1, SigE, and SigA across the whole genome of *Synechocystis*. Data in aerobic (L +O_2) and dark microoxic (D -O_2) are displayed. (B) Magnified image for chromosome position of 1,550kb-1,800kb. ChIP-seq data of cyAbrB2, cyAbrB1 , SigE and SigA in aerobic and dark microoxic conditions are overlayed. Dots below graph indicates binding region of each protein calculated by peak caller.

Figure S3

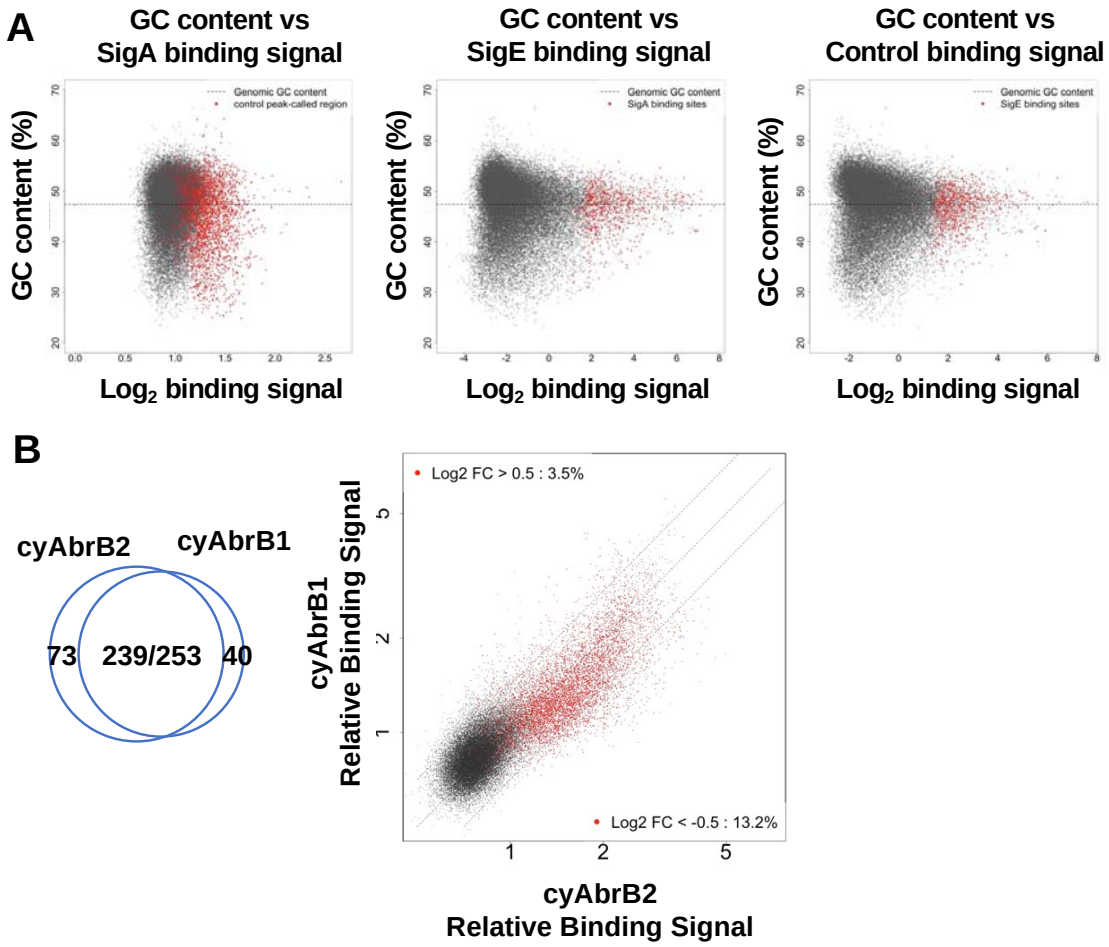

Figure S3

(A) Scatter plot showing GC contents in each 100bp vs binding signal of SigA, SigE, and control IP. Data are shown as in Figure 3C.

(B) Venn diagram showing overlap of binding region of cyAbrB1 and cyAbrB2 (left), and scatter plot showing ChIP binding signal of cyAbrB2 (y axis) and cyAbrB1(x axis) in the aerobic condition. data is plotted as in Figure 4E.

Figure S4

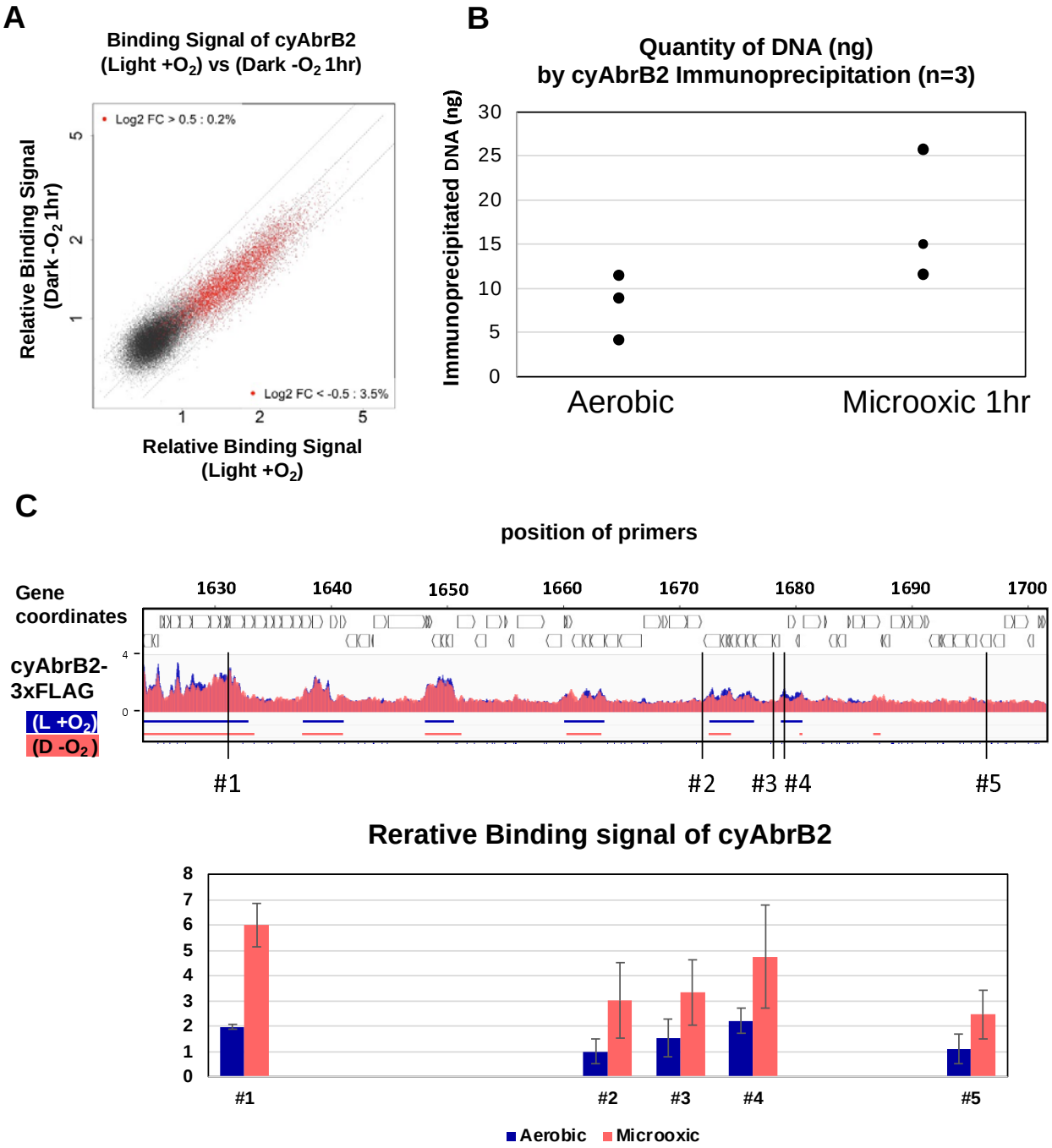

Figure S4

(A) Scatter plot showing changes of binding signal by 1hr cultivation in the microoxic condition. Binding signal of each 100bp windows are plotted. Red dots are cyAbrB2 binding region in either aerobic or microoxic condition. The dotty lines indicate Log2 fold enrichment of 0.5, 0, -0.5 between aerobic and microoxic conditions. (B) Amount of precipitated DNA by cyAbrB2 ChIP. Three experiments were performed in the aerobic and micooxic conditions. (C) Quantification for ChIP of cyAbrB2 by qPCR. The position of primers and ChIP-seq data of cyAbrB2 are shown in top.

Table S1 List of strains used in this study

Strain ID	Host strain	genotype	Reference
GT			Williams, 1988
G50	GT	*sigE*Δkm	T. Osanai, et al,2005
KR93	GT	SigA-8His-km	(Kariyazono and Osanai 2022)
KR94	GT	SigA-3FLAG-km	(Kariyazono and Osanai 2022)
KR340	GT	*abrB2*ΔKmR	in this study
KR338	GT	AbrB(sll0359)-3xFLAG-Km	in this study
KR339	GT	AbrB2(sll0822)-3xFLAG-Km	in this study

Table S2 plasmids used in this study

Plasmid ID		backbone	
VK200	AbrB1-3F-km	pTA2 (Toyobo)	transformation for KR338
VK201	AbrB2-3F-km	pTA2 (Toyobo)	transformation for KR339
VK203	abrB2Δkm	pTA2 (Toyobo)	transformation for KR340

Table S3 oligonucleotides used in this study

Oligonucleotides ID		sequence
ChIP_slr2118_F1	Figure S4C #1	CATTTCAAGCGAGATAGCAG
ChIP_slr2118_R1	Figure S4C #2	TGGAAAGTGCCTGTTCAAAG
ChIP_ThoxH_F	Figure S4C #2	CATCACCGAGGGCATATCTAG
ChIP_ThoxH_R	Figure S4C #2	ACATAAGGCTATGGAAACC
ChIP_pHox_2F	Figure S4C #3	ACAGAGGATGGACAAATGTC
ChIP_pHox_2R	Figure S4C #3	TACCGCTTCGTCATTCTGCT
ChIP_pHox_up_2R	Figure S4C #4	TCGATTACTTCCCTTTAGTG
ChIP_pHox_up_2F	Figure S4C #4	CTTCGGCTCCATGTATTC
ChIP_sll0814_F	Figure S4C #5	GTTACTACCGCTATCTATCG
ChIP_sll0814_R	Figure S4C #5	ATGACGTAAACCGGCTCTGAC